Werk

Jahr: 1983
Kollektion: fid.geo
Signatur: 8 Z NAT 2148:53
Digitalisiert: Niedersächsische Staats- und Universitätsbibliothek Göttingen
Werk Id: PPN1015067948_0053
PURL: http://resolver.sub.uni-goettingen.de/purl?PPN1015067948_0053

LOG Id: LOG_0029
LOG Titel: Archaeomagnetic investigations in Egypt: Inclination and field intensity determinations
LOG Typ: article

Übergeordnetes Werk

Werk Id: PPN1015067948
PURL: http://resolver.sub.uni-goettingen.de/purl?PPN1015067948
OPAC: http://opac.sub.uni-goettingen.de/DB=1/PPN?PPN=1015067948

Contact

Niedersächsische Staats- und Universitätsbibliothek Göttingen
Georg-August-Universität Göttingen
Platz der Göttinger Sieben 1
37073 Göttingen
Germany
Email: gdz@sub.uni-goettingen.de

J Geophys (1983) 53:131–140

Journal of Geophysics

Archaeomagnetic Investigations in Egypt: Inclination and Field Intensity Determinations

A.G. Hussain
Helwan Institute of Astronomy and Geophyscis, Helwan, Cairo, Egypt

Abstract. The intensities of the geomagnetic field (F_a), the inclinations (I) and, in one case, the declination (D) in Egypt at times between 3000 years B.C. and 1400 A.D. were determined from archaeomagnetic measurements and found to be: $F_a = 370$ to 430 μT at 3300–2900 B.C., $I = 65.1°$ to 61.2° at 1600–1450 B.C.; $F_a = 600$ μT with $I = 66.7°$ at 1400 B.C.; $F_a = 430$ μT with $I = 47.7°$ at 350–150 B.C.; $F_a = 580$ μT with $I = 45°$ at 100–50 B.C.; $F_a = 564$ μT with $I = 32.6$ and $D = -3°$ around 150 A.D.; $F_a = 372$ μT at 210 A.D.; $F_a = 540$ μT with $I = 52°$ at 1173 A.D. and $F_a = 470$ μT with $I = 54.9$ at 1450 A.D.

In order to have data and hence curves suitable for correlation with the data measured for Egypt, all the archaemagnetic data (F_a, D and I) measured from samples in an area limited by 3° East and West and 30° North of Egypt have been reduced to an Egyptian middle latitude and longitude (28.0 °W; 30.6 °E). These reduced data are in agreement with the results of this paper and with the direct observations of the geomagnetic field in Egypt during the 19th and 20th centuries.

Key words: Egypt – Archaeomagnetism – Secular variation

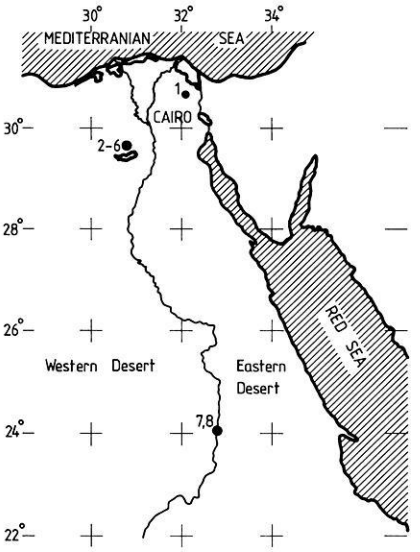

Fig. 1. A sketch map of Egypt showing the sampling sites

Introduction

Archaemagnetic data are necessary for understanding the secular variation of the geomagnetic field and could be used for evaluating different secular variation models. They also have several archaelogical applications including the possibility for use as a dating technique (Aitken, 1974).

The conditions for the study of the secular variation of the geomagnetic field from archaeological samples are better in Egypt than elsewhere, since the historical archaeological record from pre-historic through Pharaonic, Greco-Roman and Islamic ages is well preserved due to a favorable climate and well determined ages due to the tremendous works of the institutions of Egyptology all over the world. Only few archaeomagnetic studies, however, have been done in Egypt (Athavale, 1969; Games, 1980).

For this study samples were collected from Monshaat Abu Omar (3100–2990 B.C.), Madi (1800–1500 B.C. and 250–100 B.C.), Kiman Faris (1400 B.C. and 150 B.C.), Kom Oushim (150 A.C.) and Simon Bin Hadra and Matta Monastries (1200–1400 A.C.). Figure 1 is a sketch map showing these localities (for more details see Tables 1–4).

Present address: Institut für Allgemeine und Angewandte Geophysik, Theresienstr. 41-IV, 8000 München 2

Experimental Procedure and Data Reduction

Palaeointensity

The palaeointensity measurements are often made on homogeneously burnt ceramics or bricks (e.g. Aitken, 1974). Recently Games (1980) determined the palaeointensity from fired materials and has also developed a method for determination of the ancient geomagnetic field from air dried bricks with applications to samples from Egypt. He claimed that his method reached the same results as from fired materials. For the present paper we collected ceramic and brick samples from archaeologically well dated areas. Most of the ceramic samples are from thick walls of wheat containers and oven plates with thicknesses more than one inch. Several samples were cored from each sherd or brick and cast in plaster of Paris if necessary. The cylindrically shaped samples have a typical diameter of 2.5 cm, thicknesses of 0.8–2.45 cm and weights of 5–17.8 grams. A coordinate system was set up on each sherd or brick so that all samples from a sherd or a brick could be oriented relative to one another to within less than ±2°. This provides a mean

Table 1. The palaeointensity of the geomagnetic field in Egypt

Site	Location		Sample Nr.	Age years	Temp. interval °C	n	r^2	F_a in 10^{-1} mT	F_a	F_a/F_p	VDM in 10^{22} A m^2
Monshaat Abu Omar	30.8°N 32.0°E	ceramic	147-4/2	3100 B.C.	150–500	10	0.93	0.424	0.43	1.02	10.0
		ceramic	147-4/2	3100 B.C.	0–500	10	0.92	0.424			
		ceramics	147-4/3	3100 B.C.	0–500	10	0.92	0.456			
		ceramics	298/2	3300 B.C.	0–550	11	0.94	0.448	0.46	1.08	10.54
		ceramics	298/3	3300 B.C.	0–550	11	0.98	0.472			
		ceramics	127-10/1	3000–3100 B.C.	150–500	8	0.99	0.345	0.37	0.87	8.29
		ceramics	127-10/2	3000–3100 B.C.	150–500	8	0.99	0.396			
		ceramics	642/1	3300–2900 B.C.	250–550	6	0.98	0.376	0.38	0.88	8.51
		ceramics	642/2	3300–2900 B.C.	200–550	7	0.98	0.375			
Kiman Faris, Fayoum	29.5°N 30.6°E	ceramics	KF/3/Sh	1400–1350 B.C.	50–550	11	0.99	0.584	0.60	1.41	10.2
		ceramics	KF/2/Sh	1400–1350 B.C.	0–550	12	1.0	0.584			
		ceramics	KF/5/1	1400–1350 B.C.	0–550	12	0.97	0.632			
		bricks	KF/1/2-1	100–50 B.C.	0–550	11	0.99	0.608			
		bricks	KF/1/2-4	100–50 B.C.	0–550	12	1.0	0.576			
		bricks	KF2/3/2-2	100–50 B.C.	100–550	10	0.99	0.552	0.58	1.36	11.45
		bricks	KF2/3/2-3	100–50 B.C.	0–550	12	0.99	0.592			
		ceramics	KF/3/Sh	1400–1350 B.C.	50–550	11	0.99	0.584	0.60	1.41	10.2
		ceramics	KF/2/Sh	1400–1350 B.C.	0–550	12	1.0	0.584			
		ceramics	KF/5/1	1400–1350 B.C.	0–550	12	0.97	0.632			
		bricks	KF/1/2-1	100–50 B.C.	0–550	11	0.99	0.608			
		bricks	KF/1/2-4	100–50 B.C.	0–550	12	1.0	0.576			
		bricks	KF2/3/2-2	100–50 B.C.	100–550	10	0.99	0.552	0.58	1.36	11.45
		bricks	KF2/3/2-3	100–50 B.C.	0–550	12	0.99	0.592			
		bricks	KF5/3/2	100–50 B.C.	0–550	12	0.99	0.576			
		bricks	KF3/4/5	350–150 B.C.	350–550	5	0.95	0.496			
		ceramics	KF3/7/1	350–150 B.C.	200–550	8	0.97	0.400	0.43	1.01	8.11
		ceramics	KF3/7/2	350–150 B.C.	200–550	8	0.95	0.408			
Kom Oushim Fayoum	29.54°N 30.6°E	bricks	KO5/3/2	128–159 A.D.	50–550	11	0.99	0.536	0.52	1.21	11.55
		bricks	KO5/3/7	128–159 A.D.	150–550	10	0.99	0.515			
		bricks	KO7/5/1	117 A.D.	0–550	12	0.98	0.646	0.646	1.5	13.86
		bricks*	KO7/10/2	210 A.D.	450–550	3	0.90	0.372	0.372		8.53
		ceramics	KO8/2/1	147–170 A.D.	0–550	12	0.97	0.520	0.504	1.18	
		ceramics	KO8/2/4	147–170 A.D.	250–550	7	0.98	0.488			
		bricks	KO6/7/1	117–200 A.D.	200–550	8	0.98	0.589			
		bricks	KO6/7/6	117–200 A.D.	200–550	8	0.97	0.612	0.608	1.40	10.4
		bricks	KO6/7/7	117–200 A.D.	150–550	8	0.98	0.623			
		ceramics	KO8/1/1	147–170 A.D.	100–550	10	0.99	0.549	0.562	1.31	12.7
		ceramics	KO8/1/2	147–170 A.D.	150–550	9	0.99	0.576			
Anba Simon Bin Hadra Monastry	24.0°N 32.8°E	bricks	Had 1/1	1173 A.D.	0–600	13	0.97	0.504	0.54	1.26	10.2
		bricks	Had 1/3	1173 A.D.	0–550	11	0.98	0.544			
		bricks	Had 2/1	1173 A.D.	0–600	12	0.99	0.528			
		bricks	Had 2/2	1173 A.D.	100–500	9	0.98	0.542			
		bricks	Had 3/2	1173 A.D.	100–550	10	0.96	0.512			
		bricks	Had 3/4	1173 A.D.	0–600	11	0.99	0.563			
		ceramics	Had 4/2	1173 A.D.	100–550	10	0.97	0.536			
		ceramics	Had 4/6	1173 A.D.	100–550	10	0.99	0.568			
Anba Matta El-Miskin Monastry	24.0°N 32.8°E	ceramics*	Mat 1/1	ca. 1450 A.D.	150–575	9	0.97	0.616	0.61	1.42	10.4
		ceramics*	Mat 1/6	ca. 1450 A.D.	100–450	8	0.99	0.599			
		bricks	Mat 2/1	ca. 1450 A.D.	150–600	7	0.97	0.384			
		bricks	Mat 2/3	ca. 1450 A.D.	200–550	8	0.98	0.446			
		bricks	Mat 3/1	ca. 1450 A.D.	0–600	13	0.98	0.472			
		bricks*	Mat 3/4	ca. 1450 A.D.	150–550	9	0.99	0.575			
		bricks	Mat 4/2	ca. 1450 A.D.	150–550	9	0.98	0.434	0.47	1.10	9.6
		bricks	Mat 4/3	ca. 1450 A.D.	100–600	10	0.97	0.512			
		bricks	Mat 5/1	ca. 1450 A.D.	150–600	11	0.94	0.528			
		bricks	Mat 5/6	ca. 1450 A.D.	0–600	13	0.94	0.536			
		bricks*	Mat 5/7	ca. 1450 A.D.	200–550	8	0.97	0.616			

n = Number of data used for NRM versus PTRM plots; r = Standard deviation; F_a = Ancient field intensity; F_p = Present field ($= 0.427 \times 10^{-1}$ mT); VDM = Virtual dipole moment; * = The result is not consistent

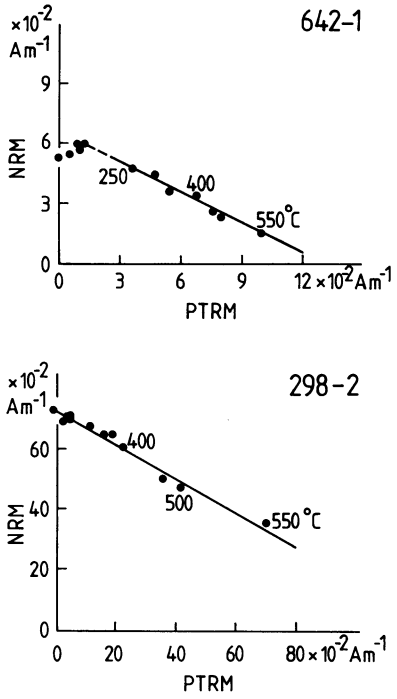

Fig. 2. NRM versus PTRM plots for two samples from Monshaat Abu Omar (3300–2900 B.C.). *Full line*: least square fit

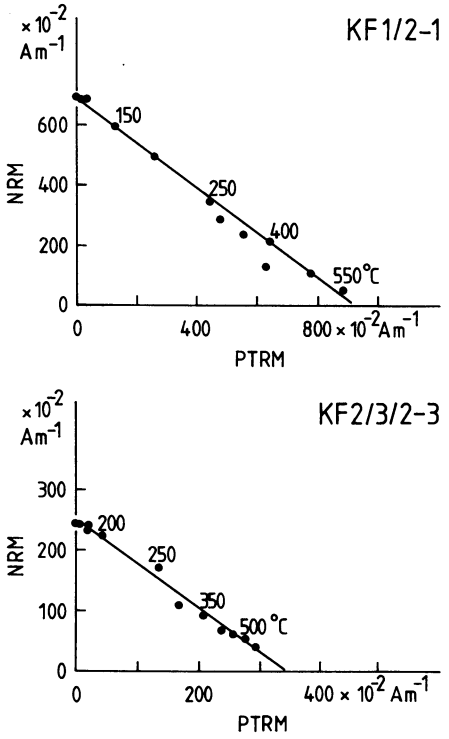

Fig. 3. NRM versus PTRM plots for two samples from Kiman Faris. *Full line*: least square fit

for checking the directional consistency of magnetization for samples from the same sherd or from the same brick. A double heating palaeointensity experiment (Thellier and Thellier, 1959) is used: A coordinate system is given to the sample. The sample is heated to a temperature I in a Schonstedt non-magnetic furnace and held at that temperature for 30 min. The sample is then shifted within few seconds to a cooling chamber with laboratory field F_{lab} of known strength and direction exactly parallel to one of the coordinates of the sample (e.g. Z-axis). After cooling to room temperature within 30–45 min while holding the sample in F_{lab} the magnetization is then measured. This magnetizations:

$J+(T)=J_{NRM}(T)+J_{PTRM}(T, T_0)$;
where T: maximum heating temperature
and T_0: room temperature.

The sample is then reheated to T and cooled in F_{lab} but with the direction of the field reversed by 180°, while the sample direction remains constant. The magnetization is again measured and then:

$J-(T)=J_{NRM}(T)-J_{PTRM}(T, T_0)$.

Vector addition and subtraction of the two measurements at the same T yield the natural remanent magnetization NRM(T) remaining after heating to T and the partial thermoremanent magnetization PTRM(T, T_0) gained by cooling from T to room temperature T_0 in the presence of F_{lab}. All heating is done in air. If NRM is plotted against PTRM (each point corresponding to a particular temperature), the result is a linear relationship (Figs. 2 to 6). The palaeointensity F_a is given by:

$F_a=-b\,F_{lab}$;
where b is the (negative) slope of the straight line.

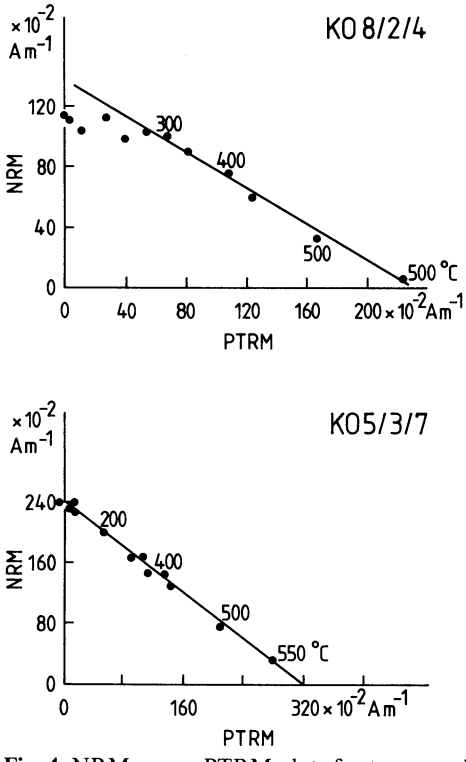

Fig. 4. NRM versus PTRM plots for two samples from Kom Oushim. *Full line*: least square fit

$F_{lab}=0.8\times10^3$ A m^{-1} has been used throughout the experiments. The samples were generally heated in successive steps of 50 °C up to 550–650 °C. Most of the NRM-PTRM plots were linear over a large part of the entire temperature range used, mainly between 150 and 550 °C. Possible causes

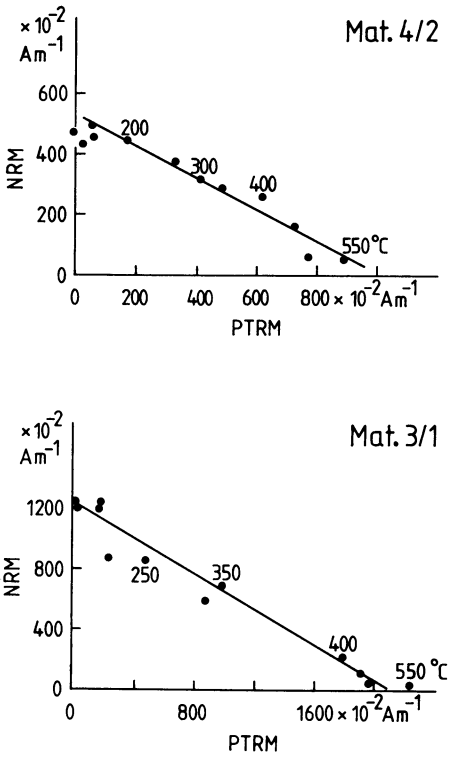

Fig. 5. NRM versus PTRM plots for two samples from Matta El Meskin Monastry. *Full line*: least square fit

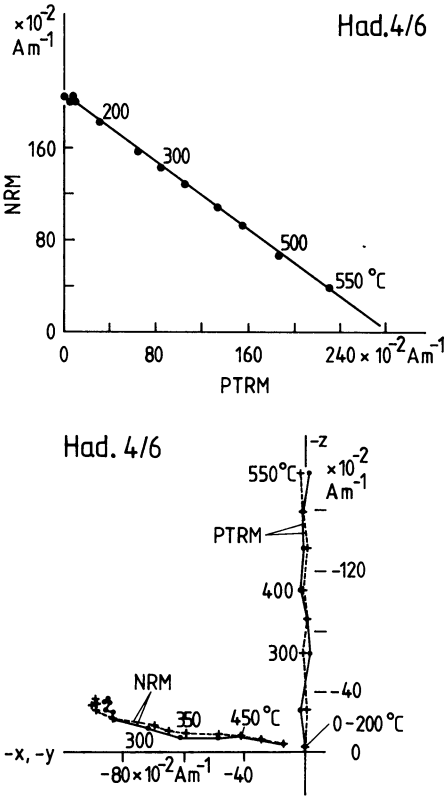

Fig. 6. *Upper part*: An example for NRM versus PTRM plots for a sample from Simon Bin Hadra Monastry. *Full line*: least square fit. *Lower part*: a vector diagram showing the variation of PTRM and NRM directions during heating and cooling processes of the same sample. All data are accepted

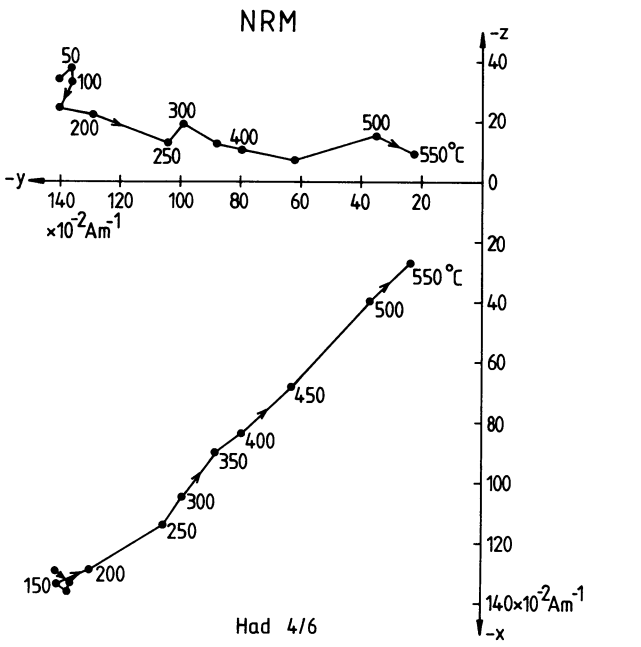

Fig. 7. Zijderveld diagram for the same sample as in Fig. 6. The viscous magnetization is negligible with respect to the NRM and hence all the data are accepted

of nonlinearity at low temperatures are viscous remanent magnetization or heating of the pottery subsequent to manufacture. Nonlinearity at high temperatures (found for only two samples at temperatures 550–650 °C) was possibly connected with a secondary chemical remanence, or with mineralogical changes during heating. Using two or three samples from the same sherd or brick is helpful in locating temperature intervals where the data appear reliable and common inflection points which might indicate a transition from useful to extraneous data. Directions of both NRM and PTRM with increasing temperature during the palaeointensity experiment were also noted and used in selection of the appropriate data subset. The samples were cooled from temperatures of more than 300 °C to room temperature in 45 min which means that the rate of cooling is much more than the possible rate during manufacture. This may lead to an overestimation of the palaeointensity of about 10–15%, sometimes even to 25% (Fox and Aitken, 1980; Walton, 1982). However, systematic investigations of that kind have not been made with the material which we used.

Figures 6 to 10 show vector diagrams of these directions. The directions of PTRM are always along the Z-axis (direction of F_{lab}) while the directions of NRM tend always towards the zero point. The viscous magnetization has been cleaned at temperatures between 50 and 200 °C (Figs. 7 and 9).

The slope of the NRM versus PTRM plots and hence the palaeointensity is determined by a least squares method. We used a least squares method where both ordinate and absissa have the same weighting for each data point. The virtual dipole moment (VDM) was calculated as:

$$\mathrm{VDM} = \tfrac{1}{2} F_a R^3 (1 + 3\cos^2 I)^{1/2};$$

where R is the Earth's radius ($= 6.371 \times 10^6$ m),
I is the inclination of the geomagnetic field at the respective ages and F_a is the field intensity measured (Table 1).

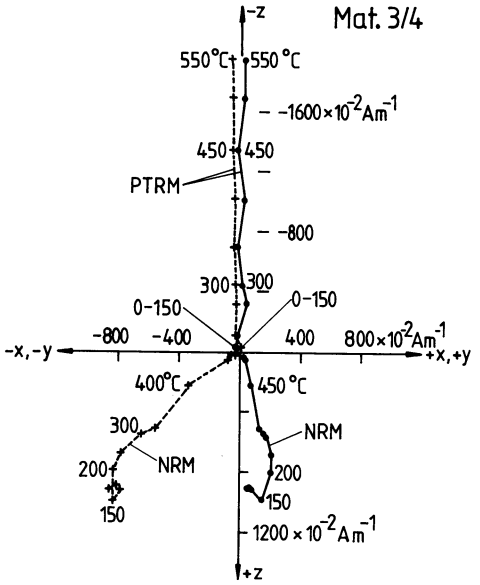

Fig. 8. Vector diagrams of PTRM and NRM for a sample from Matta El Meskin Monastry. *Crosses*: *Y–Z* plots, *points*: *X–Z* plots

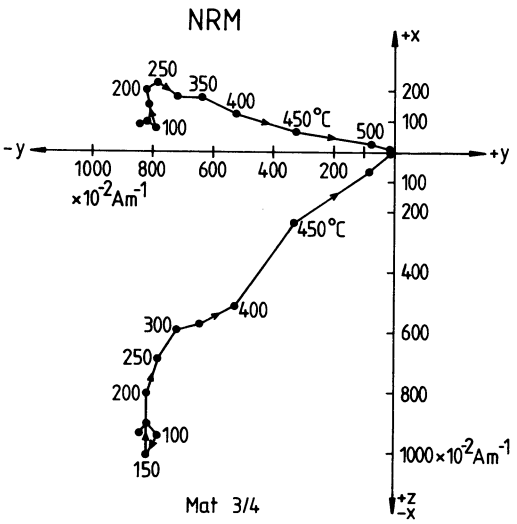

Fig. 9. Zijderveld diagram for the same specimen as in Fig. 8. The viscous magnetization as been removed at temperatures between 200 and 250 °C

The results of the palaeointensity measurements are summarised in Table 1 and represented in Fig. 11a, b.

Measurements of Susceptibility and Anisotropy of Susceptibility

Rogers et al. (1979) have claimed that ceramics possess an anisotropy of susceptibility with maximum parallel and minimum perpendicular to the wall of a ceramic sherd. Therefore, one has to pay attention to whether the magnetization of a sample in one direction is different from that in the other and hence the measured palaeointensity. To overcome this difficulty we collected the samples from thick ceramics and bricks. The susceptibilities then measured using a susceptibility bridge for all samples cored out of the sherds and bricks. These measurements were made along two perpendicular axes for each sample. The susceptibilities

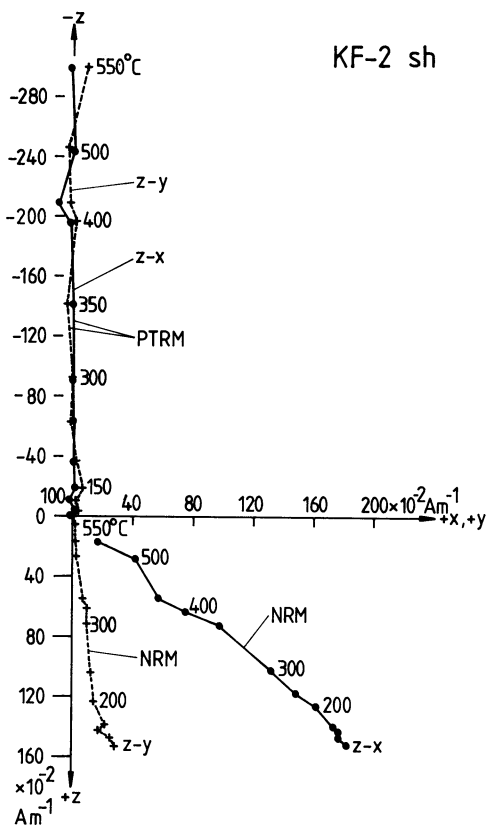

Fig. 10. Vector diagrams for the PTRM and NRM for a sample from Kiman Faris. No viscous magnetization is observed. *Crosses*: *Y–Z* plots, *points*: *X–Z* plots

of samples taken from a sherd do not differ too much from each other (see Table 2) and they seem to be isotropic. Later, some pilot samples were also subjected to anisotropy of susceptibility measurements using a Kapa-bridge type KLY-2 which is of much higher sensitivity and no effective anisotropy has been measured (Table 2). This may indicate that such thick ceramics and bricks do not possess significant anisotropy of susceptibility as detected by Rogers et al. (1979) and that it is preferable to carry out the palaeointensity measurements using such thick ceramics and bricks.

Palaeoinclination Measurements

These measurements are only possible when ceramic sherds are parts of specially shaped pottery. We collected about ten samples from each age such as parts from oven plates, large and wide fired containers, vases of large dimensions and special forms and the like. Field evidence and ornamentation lead the archaeologists and ceramicists, who were present during sampling, to the conclusion that these objects must have been baked standing upright on a horizontal surface. Bricks have been collected from buildings of known ages. The inclination could be also measured from bricks because of the regular way in which they were stacked while being baked.

In laboratory work, these sherds and bricks have been placed in positions representing exactly their positions during baking and then cast in plaster of Paris. A coordinate system was assigned to each sample. Cylindrical samples of 2.5 cm diameter were then cored from these samples and

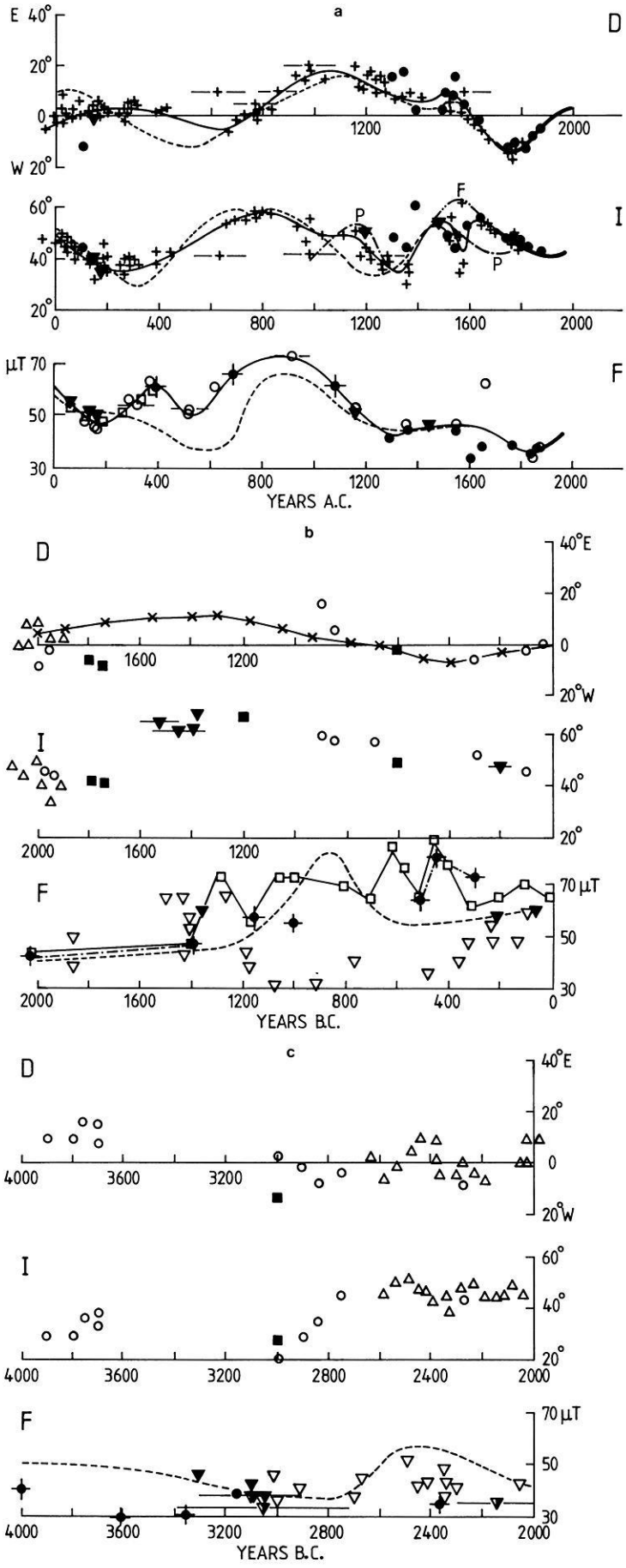

Fig. 11a–c. All the data reduced to Egypt and the results of this paper are represented in these Figures. **a** for the time interval zero A.D. to present, **b** for zero to 2000 years B.C. **c** for the time interval from 2000–4000 B.C. The letters at the side of each Figure denote: *D*: Declination (*upper part* of the curves; *E* = East and *W* = West). *I*: Inclination (*middle part* of the Figures), *F*: Palaeointensity (*lower part*). Thick lines at the end of **a** represent the observations in Egypt in the 19th and 20th centuries (Fahim and Gouda Hussain, 1977), *solid circles*: data reduced from Etna (Tanguy 1970, 1975), *open circles*: data reduced from South-Eastern Europe (Kovacheva 1976, 1977; Kovacheva and Veljovich, 1977), *solid squares*: data reduced from Turkey (Becker, 1979), *open squares*: data reduced from Athens (Walton, 1979), *solid triangle with downward head*: results of this paper, *open triangle with downard head*: data for Egypt (Games, 1980), *half open triangle with head downward*: data for Egypt (Athavale, 1969), *open triangle with upward head*: data reduced from Iran (Kawai et al., 1972), *crosses*: data reduced from Western Europe (Thellier, 1981), *crosses with solid circles*: data reduced from Ukraine and Moldavia (Rusakov and Zagniy, 1973a, 1973b), *continuous curve with "x"*: data reduced from England (Thompson, 1973), *P* in the middle part of **a**: this curve reduced from Poland (Czyszek 1976), while *F*: this part of the curve is after Thellier (1981). The continuous curves of **a** (upper, middle and down) represent the reduced data of the secular variation for Egypt during the last 2000 years

Table 2. Magnetization, susceptibility and anisotropy of susceptibility measurements

Sample No.	Type	$\bar{J}$ 10^{-5} A m^2 kg^{-1}	n	σ_J	$\bar{x}$ 10^{-9} m^3 kg^{-1}	σ_x	Anisotropy of susceptibility measurements (normalized)			
							X	Y	Z	Remarks
Mat 1	cer.	24.9	10	1.4	415.9	15.1				(1)
Mat 2	br.	33.5	10	3.5	128.2	10.1		1.03	0.98	(2)
Mat 3	br.	87.2	8	9.7	276.5	15.1		0.98	1.04	(2)
Mat 4	br.	47.3	7	7.6	272.7	12.6	1.003	1.001	0.996	(3)
Mat 5	br.	143.4	13	5.7	324.2	15.1				(1)
Had 1	br.	73.7	14	3.9	426.0	18.8	1.010	1.003	0.987	(3)
Had 2	br.	90.5	8	6.9	661.0	18.8				(1)
Had 3	br.	43.0	5	5.3	338.0	15.1				(1)
Had 4	cer.	9.3	5	0.8	125.7	8.8	1.011	1.024	*0.964*	(3)
Had 5	cer.	30.4	2	–	287.8	–		1.02	*0.98*	(2)
KO 5-3	br.	15.4	15	0.9	123.2	18.8				(1)
KO 6-5	br.	9.9	2	–	39.0	–	1.002	0.993	1.005	(3)
KO 6-7	br.	9.7	16	2.8	228.7	20.1				(1)
KO 7-10	br.	10.3	7	1.2	227.5	8.8				(1)
KO 8-2	cer.	14.2	4	–	170.9	–		1.02	*0.98*	(2)
KO 8-3	cer.	7.5	8	0.5	84.2	7.5	0.967	0.966	*1.087*	(3)
KF 2-Sh	cer.	16.0	4	0.8	145.8	8.8				(1)
KF 3-Sh	cer.	16.6	22	0.8	118.2	10.1				(1)
KF 4-1	cer.	38.4	2	–	561.7	–	1.042	0.979	*0.979*	(3)
KF 3-7	cer.	20.0	5	1.1	372.0	12.6				(1)
KF 1-2	cer.	38.0	5	2.2	366.9	11.3				(1)
KF 5-2	br.	17.6	4	1.2	51.5	7.5	1.008	0.985	1.007	(3)
M 2-3	cer.	22.1	3	–	601.9	–	1.005	1.032	*0.982*	(3)
M 4-5	br.	12.3	5	0.4	168.4	10.1	0.994	1.007	1.000	(3)

$$\sigma_J \text{ and } \sigma_\Omega = \sqrt{\frac{\sum_{i=1}^{n} (\bar{x} - x_i)^2}{n(n-1)}};$$

where $\bar{x}$ is the mean value of specific magnetization $\bar{J}$ and specific susceptibility $\bar{x}$, resepctively and x_i represents the individual values of J and x, repectively.

(1) The susceptibility was measured using a susceptibility bridge along three axis (X, Y and Z; whereas the Z axis is along the axis of the cylindrical sample). No anisotropy of susceptibility was observed.

(2) The sample were cored parallel to the wall of the sherd and perpendicular to it. The susceptibility was then measured using the same bridge as in (1).

(3) The anisotropy of susceptibility was measured using a Kapa-bridge type KLY-2.

Minimum susceptibility is in the direction perpendicular to the wall (underlined values in columns 8 to 10; these values are normalized i.e. divided by the mean value). Anisotropy of susceptibility ranges between zero and 12%

cut into specimens of 2.5 cm length. The directions of magnetization were then measured using a spinner magnetometer. The directions of magnetization of samples from a sherd or a brick were compared and found to possess small angles of confidence. Table 3 summarizes these measurements and they are represented in Figs. 11 a–c.

Other Measurements of Directions (D and I)

Samples were collected from some ovens in Karanis (Kom Oushim), Fayoum. These samples were oriented prior to removal by an exactly horizontal surface of plaster of Paris and the magnetic North was then marked on this surface. These samples were then cast in plaster of Paris and cut into cubes of 6 cm length. The directions of magnetization (both D and I) were measured using a special type of large-sample spinner magnetometer. All samples are from only one age (150 years A.C.). Table 4 contains the results of these measurements and the mean value of the direction of the geomagnetic field in Egypt at this age. This is also represented in Fig. 11 a.

Discussion

In this work, we tried to have the best conditions suitable for determination of the palaeointensities and palaeoinclinations of the geomagnetic field from archaeomagnetic measurements. The archaeological sites, from which the samples were collected, have been thoroughly studied by Egyptologists and ceramicists (e.g. Boak et al., 1931, 1933; Bresciani, 1968 and others). This enabled the trained archaeologists, who accompanied us during sampling, to determine the ages of these samples (specially with the aid of ceramicists) with an accuracy of a few tens of years. We have been able to select the most proper samples suitable for these measurements from a large variety of ceramic material. The thick ceramic sherds and bricks were found to possess negligible anisotropy of susceptibility and they are of homogeneous magnetization and susceptibility (Table 2) and hence they are the most suitable material for palaeointensity measurements.

Only one sample out of 50 was found to have nonlinearity of NRM versus PTRM plots. The vector diagrams repre-

Table 3. Palaeoinclinations of the geomagnetic field in Egypt

Location	Sample Nr.	Ages		$\bar{I}$	n	α_{95}	k	Reliability factor
Kom	5/3	147–	br.	36.0	19	1.2	699.4	a
Oushim	6/7	170	br.	37.3	17	0.9	1,537.6	a
29.54°N	6/5	A.D.	br.	25.0	2	–	–	a–c
30.6°E	8/1		cer.	33.6	6	1.5	1,422.8	a
	8/2		cer.	28.5	4	3.6	298.3	b
	7/10		br.	33.4	7	7.1	55.9	a–b
	7/5		br.	30.0	4	3.9	327.5	a–b
	11		br.	24.1	7	10.1	38.1	c
	8/3		cer.	34.3	8	3.3	286.1	a–b
	1/1		br.	32.3	15	1.5	586.5	b
	2/1		br.	22.7	15	1.9	399.8	b
	3/1		br.	29.2	10	4.4	95.6	b
	7/4		br.	41.7	1	–	–	c–d
Mean of all (except those with consistency factor c and d): $\bar{I}=30.7$, $N=11$, $A_{95}=2.8$, $K=267.5$								
Kiman	3/4	150–	br.	50.6	13	1.6	642.9	a
Faris	4/3	250	br.	45.2	11	2.8	271.4	a
29.5°N	4/2	B.C.	br.	35.5	2	14.0	19.7	b–c
30.6°E	5/4		br.	45.3	4	3.0	927.2	a
	3/7		cer.	68.0	5	7.6	102.7	d
	5/8		br.	43.4	2	–	–	c
	5/6		br.	34.0	3	11.9	60.5	b–c
	5/2		br.	50.2	6	4.1	266.6	a–b
	2/3		br.	54.4	7	4.4	147.4	b
	5/3		br.	42.2	7	1.1	2,936.4	a–b
	5/1		br.	48.4	7	2.5	593.8	a
	4/1		br.	22.3	2	–	–	c–d
	1/5		br.	24.9	1	–	–	d
Mean of those with consistency factor a–c: $\bar{I}=47.7$, $N=9$, $A_{95}=2.75$, $K=406.7$								
Kiman	10	ca.	cer.	70.2	17	3.1	118.6	b
Faris	4	1400	cer.	67.8	9	4.1	128.0	a–b
29.51°N	3	B.C.	cer.	66.6	3	11.2	122.6	b
30.6°E	5		cer.	61.6	6	6.2	118.6	a–b
	7		cer.	60.8	5	11.1	48.8	b
	3/7		cer.	68.9	5	7.6	102.7	b
	1		cer.	72.5	9	3.1	118.6	c
Mean of all: $\bar{I}=66.7$, $N=7$, $A_{95}=3.2$, $K=350$								
Lahoun,	L_1	1550–	cer.	61.7	7	8.6	49.9	a
Fayoum	L_2	1350	cer.	61.6	5	3.8	414.0	a
29.53°N		B.C.						
30.6°E	Mean of L_1 and L_2: $\bar{I}=61.7$							
Biahmo,	B_2	1550–	cer.	60.3	4	4.2	472.1	a
29.48°N	B_5	1350	cer.	61.7	2	–	–	b
30.59°E		B.C.						
Mean of B_2 and B_5: $\bar{I}=61.2$								
Madi,	2/1	1600–	cer.	66.2	12	4.3	90.0	a
Fayoum,	2/10	1450	cer.	73.4	4	2.0	1,267.1	a–b
29.47°N	1/5	B.C.	cer.	68.2	4	3.8	334.5	a
30.6°E	3/4		cer.	51.8	5	3.0	422.2	b
	1/3		cer.	69.8	2	–	–	b
	1/1		cer.	61.8	4	4.8	364.1	b
	3/5		cer.	56.4	4	2.4	1,426.4	a
	3/1		cer.	71.6	5	2.6	853.8	a
	2/5		cer.	74.4	4	4.5	411.2	a
	4/5		cer.	66.1	6	1.0	4,567.2	a
	4/6		cer.	59.7	2	11.8	450.4	c
Mean of all: $\bar{I}=65.1$, $N=11$, $A_{95}=4.1$, $K=125.8$								

Table 3 (continued)

Location	Sample Nr.	Ages		$\bar{I}$	n	α_{95}	k	Reliability factor
Anba	1	ca.	br.	47.6	14	1.8	409.3	a
Simon	2	1200	br.	41.0	11	1.3	1,032.0	a
Bin	3	A.D.	br.	65.4	11	1.3	1,045.9	a–b
Hadra	4		cer.	59.7	8	2.7	336.9	a–b
Monastry	5		cer.	51.5	1	–	–	c
	6		cer.	47.5	1	–	–	c
	7		cer.	51.5	6	4.0	217.3	b–c
Mean of all: $\bar{I}=52.0$, $N=7$, $A_{95}=6.1$, $K=98.8$								
Matta	1	1450–	cer.	67.1	14	1.5	588.8	a
El-	2	1500	br.	74.3	10	4.5	95.6	a–b
Meskin	3/1	A.D.	br.	47.4	8	3.3	224.2	a–b
Monastry	3/2		br.	45.7	3	3.4	561.2	b
	4		br.	58.7	8	4.8	106.6	a
	5		br.	47.2	14	1.0	1,381.0	a
	6		br.	44.8	4	1.2	3,599.0	a–b
Mean of all: $\bar{I}=54.9$, $N=7$, $A_{95}=8.9$, $K=47.1$								

$\bar{I}$ = Mean inclination measured from specimens cored out of a sample (column 5); n = Number of specimens, α_{95} and k are Fisherian statistical parameters (the directions of magnetization of specimens from a sample are nearly of the same declination, e.g. within ±2°), $\bar{I}$ mean of all samples

Table 4. Mean direction of the geomagnetic field (D and I) in Egypt at 150 years A.D. (Location: 29.5°N, 30.6°E)

Sample Nr.	$\bar{D}$ (°)	$\bar{I}$ (°)	n	α_{95}	k
KO 1	−11.2	33.2	17	3.86	86.23
KO 2	−12.7	23.4	15	7.48	27.1
KO 3	− 9.4	40.8	29	5.28	26.7
KO 8	11.7	24.3	6	4.54	218.3
KO 9	no consistent results				
KO 10	5.3	31.2	3	6.7	338.5
KO 11	no consistent results				
KO 13	−2.6	40.6	28	0.83	1,074.96
Mean of all: $\bar{D}=3.0°$, $\bar{I}=32.6°$, $N=6$, $A_{95}=9.5$, $K=50.72$					

senting the behavior of the direction of NRM and PTRM during heating and cooling processes are useful for selecting the data subset suitable for NRM versus PTRM plots. The PTRM vector diagrams (Figs. 6, 8 and 10) show that the PTRM is always parallel to the direction of F_{lab}, while the NRM vector diagrams (Figs. 6–10) are useful in determining the extraneous data subset where the viscous magnetization is effective. In most of our samples the viscous magnetizations have been removed at temperatures between 50 °C and 250 °C. Sometimes the intensity of the viscous magnetization is much smaller than the NRM so that it does not effect the linearity of the NRM versus PTRM plots.

Unfortunately no determinations have been made for the directions of the geomagnetic field in Egypt in historic times. Only two papers have been published concerning the palaeointensity of the geomagnetic field in Egypt: one by Athavale (1969) in which he measured the palaeointensity from two sample sets of uncertain ages (one for an

age between 3400–2700 B.C. and the other for an age between 2300–1700 B.C.) and the other paper by Games (1980) in which he determined the palaeointensity between 3000 B.C. and 0 B.C. using air dried bricks as well as fired ceramics and bricks. We tried to measure the magnetization of some samples from recent air dried bricks using a spinner magnetometer and we found that their magnetizations are less than 10^{-4} A m^{-1}.

To make correlations with our results, we used all the data obtained from archaeomagnetic measurements in an area close to Egypt so that the non-dipole part of the geomagnetic field can be minimized. The directions of the geomagnetic field (D and I) measured from samples from Western Europe (collected by Thellier, 1981), South-Eastern Europe (Kovacheva, 1976, 1977), Turkey (Becker, 1979), Cyprus (Tanguy, 1970), Iran (Kawai et al., 1972) and Ukraine and Moldavia (Rusakov and Zagniy, 1973a and b) were reduced to a mean site in Egypt. These pairs of archaeomagnetic D and I data together with their respective site localities (latitudes and longitudes) were used to calculate the pole positions of the geomagnetic field at their respective ages (for equations for calculating the pole position of the geomagnetic field from D, I, latitude and longitude of sampling site see, for example, McElhinny, 1973). From these pole positions the directions of the geomagnetic field (D and I) were calculated for Egypt (latitude 28.0 °N, longitude 30.6 °E). These reduced data are represented in Figs. 11 a–c.

The palaeointensities of the geomagnetic field measured at Athens (Walton, 1979), South East Europa (Kovacheva, 1977; Kovacheva and Veljovich, 1977), Ukraine and Moldavia (Rusakov and Zagny, 1973a and b), Czechoslovakia (Bucha, 1967, 1970) and Italy (Tanguy, 1975) have also been reduced to Egypt. Walton (1982) stated that his previous results are overestimated by 15–25%. However, this has no serious effect on our conclusions. The virtual dipole moment equation was used for such reduction.

$$F_{Egypt} = F_{site} \left(\frac{1 + 3\cos^2 I_{site}}{1 \times 3 \cos^2 I_{Egypt}} \right)^{1/2}.$$

These reduced palaeointensity data are represented in Figs. 11 a–c, lower parts.

The observations of the geomagnetic field (F, D and I) made in Egypt in the 19th and 20th centuries (Fahim and Gouda Hussain, 1977), represented as thick lines in the last part of Fig. 11 a, coincide with the reduced data which may indicate a suitable method of reduction. Our results from this paper are also in good agreement with these reduced data.

The periodicity of the geomagnetic field of 2800 years suggested by Thompson (1973) and Bucha (1967) cannot be seen in our data.

The secular variation curves, especially for the period zero to 2000 years A.C. (Fig. 11 a), are suitable for rough chronological estimates. Many more measurements of samples from Egypt for ages along the whole historic column are needed for the enrichment of the data and hence the production of curves suitable for chronology.

Acknowledgments. We are greatly thankful to the Egyptian archaeologists who accompanied me during sampling, specially Mr. Ali Bazeidy, inspector of archaeology of El Fayoum Area and Mr. Ahmed Mousa of Sakkara and Pyramids Areas. Thanks are also due to Dr. Strauss, Institute of Egyptology of the University of Munich for providing the samples from Monshaat Abu Omar.

The measurements were made partyly in the Institut für Allgemeine und Angewandte Geophysik, University of Munich and partyly in the Helwan Institute of Astronomy and Geophysics, Helwan, Cairo. We are thankful to Prof. Dr. G. Angenheister, Prof. Dr. H. Soffel, Prof. Dr. A. Schult and Dr. H. Becker from the first Institute and to Prof. Dr. M. Fahim, Prof. Dr. H. Deebes and Dr. A. Gh. Hassaneen from the second one. Special thanks are due to Prof. Dr. H. Soffel for kindly reading the manuscript.

References

Aitken, M.J.: Physics and Archaeology, 2nd. edt. Oxford: Clarendon Press 1974

Athavale, R.N.: Intensity of the geomagnetic field in pre-historic Egypt. Earth Planet. Sci. Lett. **6**, 221–224, 1969

Becker, H.: Archaeomagnetic investigations in Anatolia from prehistoric and hittite sites. Proceedings of the 18th. International Symp. on Archaeometry and Archaeological prospection, Archaeo-Physico **10**, 382–387, 1979

Boak, A.E.R.: Karanis, The temples, coin hoards, botanical and zoological reports, seasons 1924–1931. Univ. Michigan Press, 1933

Boak, A.E.R., Petersen, E.E.: Karanis, topographic and architectural report of excavations during seasons 1924–1928. Univ. Michigan Press, 1931

Bresciani, E.: Messione die scavo Medinet Madi (Fayoum-Egitto), Rapporto preliminiare della campagne di scavo 1966 e 1967, 1968 (also other unpublished reports of the Institute of Egyptology Univers. Milano for 1968 and 1969 from Foraboschi, D.)

Bucha, V.: Intensity of the Earth's magnetic field during archaeological times in Czechoslovakia. Archaeom. 10, 12–25, 1967

Bucha, V.: Evidence for changes in the Earth's magnetic field intensity. Phil. Trans. R. Soc. Lond. **A 269**, 47–55, 1970

Czyszek, W.: Archaeomagnetism, a preliminary report. Publ. Inst. Geophys. Pol. Acad. Sci. **76**, 59–70, 1976

Fahim, M., Gouda Hussain, A.: The secular variation of the geomagnetic field at Helwan, Egypt. Helw. Observ. Bull. **139**, 1–19, 1977

Fox, J.M.W., Aitken, M.J.: Cooling-rate dependence of thermoremanent magnetization. Nature **283**, 462–463, 1980

Games, K.P.: The magnitude of the archaeomagnetic field in Egypt between 3000 and 0 B.C. Geophys. J. R. Astron. Soc. **63**, 45–56, 1980

Kawai, N., Hirooka, K., Nakajima, J., Tokieda, K., Tosi, M.: Archaeomagnetism in Iran. Nature **236**, 223–225, 1972

Kovacheva, M.: Archaeomagnetic investigations of some pre-historic sites in Bulgaria. Archaeom. **18**, 99–106, 1976

Kovacheva, M.: Archaeomagnetic investigations in Bulgaria: Field intensity determinations. Phys. Earth. Planet. Inter. **13**, 355–359, 1977

Kovacheva, M., Veljovich, D.: Geomagnetic field variations in South-Eastern Europe between 6500 and 10 years B.C. Earth Planet. Sci. Lett. **37**, 131–138, 1977

McElhinny, M.W.: Palaeomagnetism and plate tectonics, Cambridge Uni. Press 1973

Rogers, J., Fox, J.M.W., Aitken, M.J.: Magnetic anisotropy in ancient pottery. Nature **277**, 644, 1979

Rusakov, O.M., Zagniy, G.F.: Intensity of the geomagnetic field in the Ukraine and Moldavia during the past 6000 years. Archaeom. **15**, 275–285, 1973a

Rusakov, O.M., Zagniy, G.F.: Archaeomagnetic secular variation study in the Ukraine and Moldavia. Archaeom. **15**, 153–157, 1973b

Tanguy, J.C.: An archaeomagnetic study of mount Etna: The magnetic direction recorded in lava flows subsequent to the twelfth Century. Archaeom. **12**, 115–128, 1970

Tanguy, J.C.: Intensity of the geomagnetic field from recent Italian

lavas using a new palaeointesnity method. Earth Planet. Sci. Lett. **27**, 314–320, 1975
Thellier, E.: Sur la direction du champ magnétique Terrestre en France durant le deux derniers millenaires. Phys. Earth Planet. Inter. **24**, 89–132, 1981
Thellier, E., Thellier, O.: Sur l'intensité du champ magnétique terrestre dans le passé historique et géologique. Ann. Géophys. **15**, 285–376, 1959
Thompson, R.: Palaeolimonology and palaeomagnetism. Nature **242**, 182–184, 1973
Walton, D.: Geomagnetic intensity at Athens between 200 B.C. and 400 AD. Nature **277**, 643–644, 1979
Walton, D.: Errors and resolution of thermal techniques for obtaining the geomagnetic intensity. Nature **295**, 512–515, 1982

Received November 30, 1982; Revised version March 17, 1983; Accepted April 12, 1983